Seismic Risk Mitigation for the Athenian Acropolis Wall: Structural and Geotechnical Strategies

D. Egglezos [1]

[1]PhD Civil Engineer, GEO.PER. SA, Hellenic Open University (HOU) , dimitrios.egglezos@gmail.com

ABSTRACT

The Circuit Wall of the Athenian Acropolis is a monumental masonry system that supports historic fills and, locally, behaves as a free-standing wall due to the historical removal of backfill during major excavations. Its stability is challenged by strong earthquakes and by long-term deterioration of porous stone blocks and joints. Seismic risk mitigation is therefore treated as a performance-based improvement problem under strict conservation constraints, where interventions must be compatible, durable, minimally invasive, and—where feasible—reversible (ICOMOS 1964; ICOMOS 2003; Ambraseys, 2010; Egglezos et al., 2022).

A multidisciplinary assessment is presented for eight priority areas (A1–A8) of the Circuit Wall (YSMA 2020, GEO.PER. S.A. & DOMOS S.A., 2018). The approach combines historical and archaeological documentation (Kavvadias & Kawerau, 1907; Bundgaard, 1974; Korres, 2015), with geological–geotechnical interpretation and nonlinear soil–structure interaction (SSI) modelling of representative cross-sections (Sections S1 – S21). Both two-dimensional and targeted three-dimensional models are used where geometry varies abruptly. Seismic performance is evaluated against explicit damage/performance criteria (D1–D4) linked to regulatory hazard levels (CEN, 2004a; 2004b; 2004c; OASP 2022; GEO.PER. S.A. & DOMOS S.A. 2023).

Interventions are organised as standardised bundles (B1–B8) comprising (i) selective masonry consolidation where deterioration is controlling, (ii) predominantly geotechnical measures that reduce earth-pressure demand and restore protective ground conditions while preserving gravity-retaining action, and (iii) passive protection where constraints prevent achievement of target performance. Verification analyses (representative areas) indicate substantial reductions in displacement demand and plastic/cracking zones under the extreme design earthquake for the examined configurations, while constrained areas require consequence-reduction through permanent protective measures (GEO.PER. S.A. & DOMOS S.A., 2023).

Keywords: Acropolis Circuit Wall, Ancient Retaining Structures, Passive seismic protection, Soil-structure interaction, Dry-stone masonry, Reversible strengthening techniques

INTRODUCTION

Monumental Circuit Walls differ fundamentally from conventional retaining structures: they are multi-phase assemblages with discontinuous construction logic, limited documentation of internal arrangement, and strong constraints on invasive strengthening. Their performance depends not only on global stability (sliding/overturning) but also on localized mechanisms governed by weak interfaces, thin outer leaves, backfill heterogeneity, drainage deficiency, and foundation irregularities (Bundgaard, 1974; Korres 2015)

For the Acropolis Circuit Wall, seismic risk management must operate under three simultaneous constraints:

- heritage compatibility (minimum intervention, reversibility where possible, limited visibility),

- strong spatial variability in structural typology and ground conditions along the alignment, and
- uncertainty in geometry, interfaces, and mechanical properties, which reduces the value of single "absolute" safety factors and instead favors comparative and performance-based reasoning (Korres, 2015; YSMA, 2020).

This paper presents an assessment-to-intervention workflow that uses (i) zoning into prioritized Areas (A), (ii) nonlinear SSI modeling combined with an incremental pseudo-static "pushover-like" procedure for seismic actions, and (iii) deformation-based performance criteria mapped to Damage/Performance Levels (D). The intent is to establish an internationally readable, performance-based framework that integrates observed vulnerability, identified governing mechanisms, deformation-based performance metrics, and conservation-compatible intervention bundles (Egglezos et al., 2022, GEO.PER. S.A. & DOMOS S.A., 2023, 2019; OASP, 2022).

MONUMENT AND SYSTEM DESCRIPTION

The Circuit Wall extends for more than 700 m with heights varying roughly from a few metres to nearly 20 m, founded on limestone rock and supporting historic fills of variable thickness. The wall comprises segments that function predominantly as:

- retaining walls, in which behaviour is governed by lateral earth pressures and interaction with retained backfill,
- free-standing walls, characterized by slender masonry response and significant seismic inertia effects,
- composite structural configurations combining retaining action with buttresses, local reconstructions (Figures 1-3), and heterogeneous internal construction (Korres, 2002; 2004; 2015).

Although the present contribution focuses primarily on the portions of the Circuit Wall that operate as retaining structures, the free-standing segments created by historic excavations were also examined for completeness. Their seismic behaviour was assessed through nonlinear dynamic time-history analyses using a limited set of carefully selected acceleration records compatible with the site hazard and the expected response characteristics of slender masonry. The computed deformation demand for the existing condition remained within the project's admissible performance objectives; consequently, interventions in these free-standing portions are generally confined to conservation-oriented, predominantly static measures (e.g., local re-bedding and repointing, replacement of severely weathered blocks, addition of new marerial where necessary, and discrete joint/interface detailing), rather than additional seismic upgrading systems.
Construction phases include ancient masonry (dry masonry with with large blocks), later reconstructions (usually mortared masonry) with various stone material and bonding, and localised modern interventions. The system therefore exhibits discontinuities in stiffness, mass distribution, interface quality, and rainwater-management paths (Bundgaard, 1974; YSMA, 2020).

Figure 1. *Characteristic area of the north side of the Circuit Wall, where the ancient wall and later phases intertwine*

Figure 2. *Characteristic area of the south side of the Circuit Wall, where only later phases are visible*

Figure 3. *Later stonework with mortar (reconstruction) of the eastern section of the Circuit Wall of the Acropolis) (YSMA, 2020).*

ZONING AND PRIORITISATION BY AREAS

For practical assessment and intervention planning, the wall alignment is subdivided into priority Areas A1–A8 (Figure 4), corresponding to distinct combinations of geometry, typology, foundation morphology, and documented deterioration/damage. Within each area, representative cross-sections (Sections S1 – S21) are selected to capture the range of wall height, retained soil height, structural configuration (dry-stone, rubble core, reconstructed masonry), proximity to buttresses, and local rainwater exposure (YSMA, 2020; GEO.PER. S.A. & DOMOS S.A., 2023).

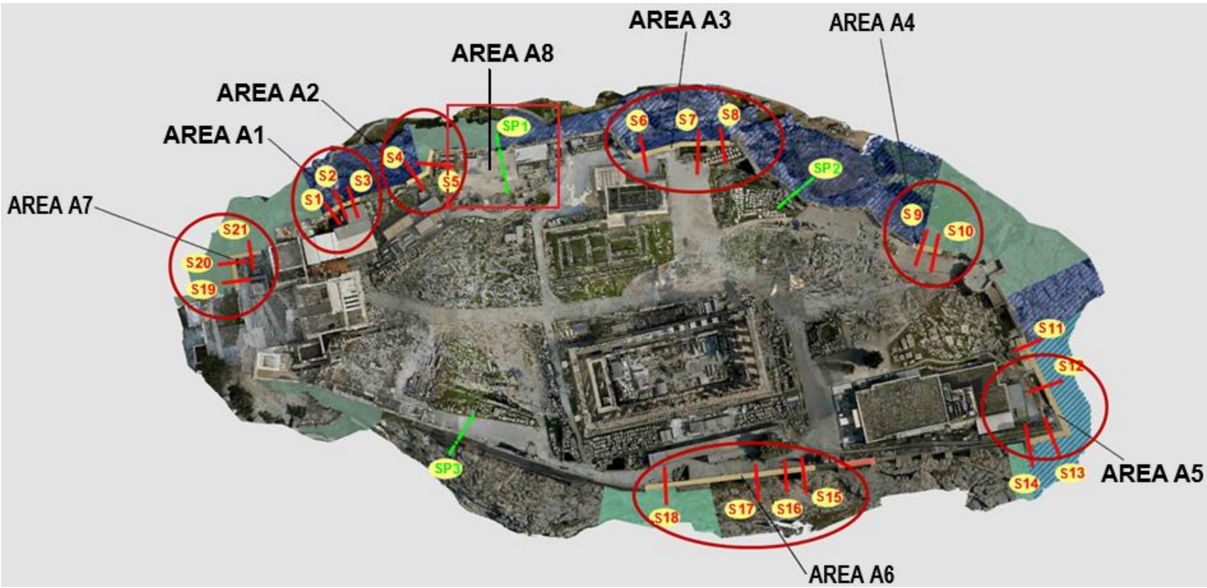

Figure 4. *Landscape of the Acropolis terrace with the 8 areas for planning measures to improve stability (YSMA 2020, GEO.PER. S.A. & DOMOS S.A., 2023).*

GOVERNING VULNERABILITY THEMES AND RESPONSE MECHANISMS

Observed vulnerability is best interpreted through mechanisms that couple masonry behaviour with geotechnical demand:

- Outward rotation / overturning tendency in retaining segments, driven by earth pressures, increased transient pore pressures from intense rainwater infiltration and temporary water accumulation behind the wall, and seismic inertia. This mechanism is naturally expressed by relative top displacement normalised by wall height (a deformation proxy for rotation) (CEN, 2004a; 2004b; GEO.PER. S.A. & DOMOS S.A., 2023).

- Base or interface sliding, especially where bedding planes, construction joints, or degraded interfaces provide low residual shear resistance. Sensitivity to interface friction is particularly important in discontinuous masonry ("discrete structure") configurations (GEO.PER. S.A. & DOMOS S.A., 2023).

- Localised cracking/plasticity in thin outer leaves or transition zones between construction phases. In nonlinear SSI modelling this manifests as plastic zones in masonry/rock materials and concentration of deformation along interfaces (GEO.PER. S.A. & DOMOS S.A., 2023).

- Rainwater-driven hydro-mechanical amplification, whereby intense short-duration rainfall combined with inadequate drainage increases lateral earth pressures and reduces effective stress at critical interfaces, resulting in a lower acceleration threshold for a given damage state. The analyses do not assume the existence of a permanent groundwater table. (GEO.PER. S.A. & DOMOS S.A., 2023).

These mechanisms are clarified through the analysis outputs (permanent displacement, interface slip, plastic zones) and lead to the selection of appropriate interventions as mechanism-targeted bundles (GEO.PER. S.A. & DOMOS S.A., 2023).

ASSESSMENT METHODOLOGY

Modelling concept and constitutive assumptions

Two-dimensional (2D) SSI modelling is adopted as a practical representation of the wall–fill–rock system along most of the alignment, where plane-strain conditions are typically dominant. The underlying geotechnical report describes 2D elastoplastic pseudo-static SSI analyses using a combination of finite elements and distinct/discrete element logic to represent discontinuous structural behaviour in gravity walls (GEO.PER. S.A. & DOMOS S.A., 2023).

The analyses were conducted within the regulatory framework of Eurocode 7 (CEN, 2004a) and Eurocode 8 (CEN, 2004b; 2004c), under a seismic action corresponding to a return period of TR = 1300 years.
The 2D nonlinear pseudo-static soil–structure interaction analyses were carried out using PHASE2 Version 8 (Rocscience Inc., 2014). The nonlinear dynamic analyses (2D dynamic cross-check analyses of representative sections and full 3D required for areas with abrupt geometric changes and non-plane-strain behaviour) were carried out using RS3 software (RocScience, 2023) and were verified with MIDAS software.
In the present analyses, the following constitutive idealisations were adopted (GEO.PER. S.A. & DOMOS S.A., 2023):

- Fills/backfills: elastoplastic Mohr–Coulomb behaviour (Duncan & Wright, 2005).

- Foundation rock: elastoplastic Hoek–Brown representation with consistent rock-mass quality assumptions (Hoek, 1980; Hoek, 2000, Hoek 2002).

For the wall body, the constitutive idealisation depends on the construction typology. In the ancient dry-stone masonry zones, the stone blocks are represented as deformable bodies governed by the Hoek–Brown criterion, whereas the dry joints between adjacent blocks are represented by Mohr–Coulomb interface elements with frictional behaviour and without cohesion or tensile strength, so as to capture joint opening, sliding, and local loss of contact. In the later mortared rubble masonry zones, a plausible idealised stone skeleton is introduced on the basis of the typical stone sizes and masonry texture, with each stone represented as a distinct block separated from the adjacent ones by mortar-defined interface boundaries. The stone units are again modelled with the Hoek–Brown criterion, while the mortar joints are represented by Mohr–Coulomb interface elements characterised by normal and shear stiffness and by strength parameters comprising cohesion, friction angle, and tensile strength. In this idealisation, the mortar is treated as an interface material governing bond, sliding resistance, and opening between adjacent stones; therefore, its compressive behaviour is not introduced as an independent input parameter, but is reflected indirectly through interface opening and closure and the increase of shear resistance under compressive normal stress. It should be noted that, for mortared masonry, an alternative equivalent-continuum idealisation could also be adopted, whereby the assemblage is represented as a homogeneous material governed by appropriately calibrated Hoek–Brown parameters. Although such an approach may be suitable for more uniform, quasi-monolithic mortared masonry, it was not selected in the present study, because the later mortared masonries of the Acropolis Circuit Wall were considered to be more realistically represented by distinct stones separated by mortar interfaces. In addition, indicative axisymmetric numerical tests on a representative stone specimen were used as supporting checks of the adopted Hoek–Brown response at unit level (Fig. 5). Representative geometric and structural data, the adopted 2D SSI discretisation, and a typical historical embankment view are shown in Figures 6–8, respectively.

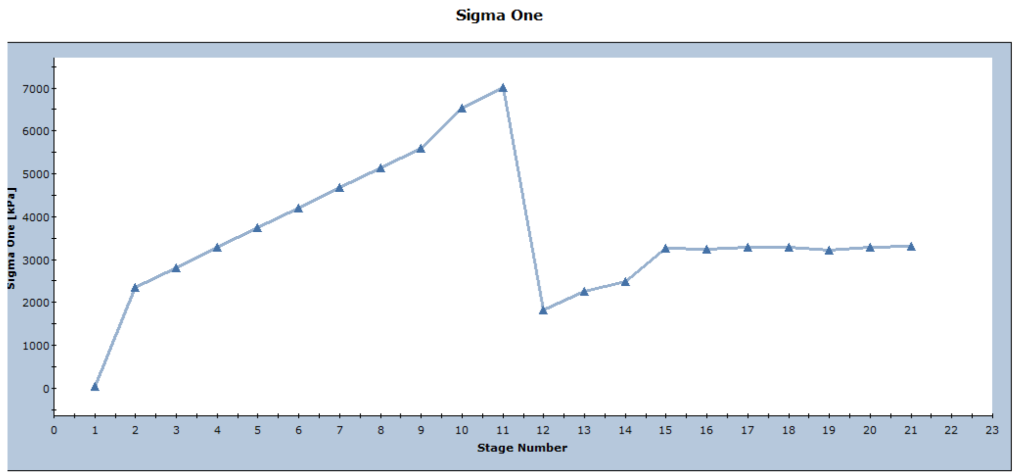

Figure 5. *Indicative plot from the axisymmetric Hoek–Brown numerical test on a representative stone specimen, used as a supporting unit-level check of the adopted stone-block response.*

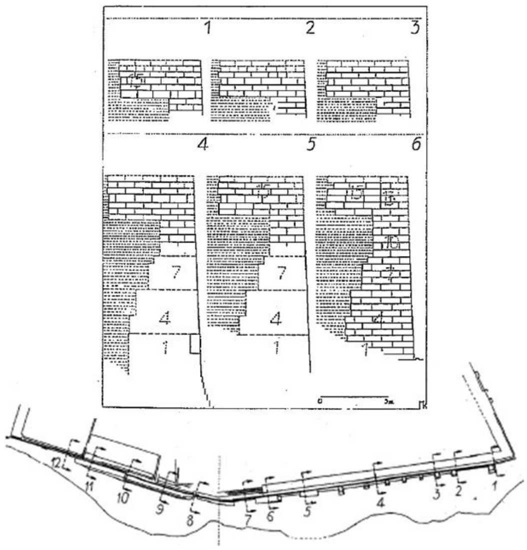

Figure 6. Characteristic geometric structural data of the eastern branch of the South Wall of the Acropolis (Section and plan from M. Korres' Drawings).

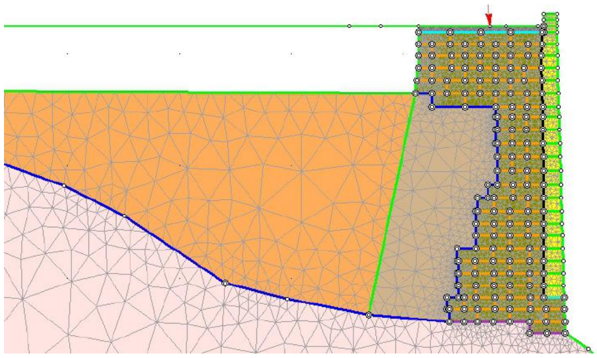

Figure 7. Schematic of the 2D SSI modelling domain and typical discretisation: rock foundation, backfill, wall body, and explicit interfaces for discontinuous masonry segments.

Figure 8. Typical view of the classical artificial embankments for the creation of the Acropolis terrace (photo from the major excavation: 1885 – 1891) (archives of YSMA).

Performance criteria and Damage Levels (D)

Performance classification is based on deformation measures rather than a single "true" factor of safety. Deformation measures are mapped to Damage/Performance Levels D1–D4, defined separately for retaining-type and free-standing-type behaviour:

- K1-type (retaining behaviour): relative top displacement with respect to the base, normalised by wall height (Egglezos et al., 2022)

- K2-type (free-standing behaviour): relative displacement of the wall crest with respect to its base, normalised by the wall base width (, which provides a practical proxy for overall equilibrium (i.e., incipient loss of stability/rocking). (Egglezos et al., 2022).

Threshold ranges for the K1-type and K2-type criteria are presented in Table 2 *(*Egglezos et al., 2022; GEO.PER. S.A. & DOMOS S.A., 2023*).*

Table 2. *Performance criteria and Damage Levels (D1–D4) used for classification of response in retaining and free-standing conditions (thresholds for normalised top displacement) (Egglezos et al., 2022; GEO.PER. S.A. & DOMOS S.A., 2023).*

K1-type criterion	
Normalized (by Height) Relative Roof-to-Base Drift	**Performance Level – Limit State**
< 2%	D1 – Almost full functionality
2% – 5%	D2 – Limited damage
5% – 10%	D3 – Significant damage
10% – 15%	D4 – Near collapse
K2-type criterion	
Normalised by the wall base width displacement of the wall crest	
< 15%	D1 – Almost full functionality
15% – 35%	D2 – Limited damage
35% – 50%	D3 – Significant damage
>50%	D4 – Near collapse

Earthquake action as incremental pseudo-static "pushover-like" procedure

Earthquake demand is introduced through pseudo-static loading in which a control horizontal acceleration is incremented until a computational limit state is reached. In the underlying geotechnical report, both SSI analyses and limit-equilibrium analyses were executed per cross-section with acceleration scaling from 0.02 g upward, using an increment Δa = 0.02 g, until "computational seismic failure" (GEO.PER. S.A. & DOMOS S.A., 2023).

This incremental procedure provides capacity-type curves linking acceleration demand to deformation response and supports ranking of sections by the acceleration at which D-level thresholds are reached. A characteristic presentation of the resulting incremental pseudo-static performance mapping is shown in Figure 9.

The regulatory framework for the analyses and result interpretation were Eurocodes 7 and 8 (CEN 2004a; 2004b) and the Greek Code of Assessment and structural Intervention on masonry buildings (OASP, 2022). Similar to the 2D pseudo-static analyses for the estimation of the current condition of the Circuit Wall, the regulatory seismic event for the design of measures is T_R=1300 years.

Area	Cross-Section		NSL [1]	HHL [2]	Earthquake Load - a_h (g), a_v=a_h/2															
					0,02	0,04	0,06	0,08	0,10	0,12	0,14	0,16	0,18	0,20	0,22	0,24	0,26	0,28	0,30	0,32
A2	S4	RD[3] (%)	0,00	0,00	0,02	0,03	0,05	0,07	0,1	0,19	0,3	0,51	1,1	3,8	5,48	8,18	11,27			
		PL[4]	D1	D1	D1	D1	D1	D1	D1	D1	D1	D1	D1	D2	D3	D3	D4			
	S5-inner	RD[3] (%)	0,00	0,02	0,03	0,05	0,1	0,14	0,24	1,61	2,67	2,42	3	3,64	4,51	5,6	7,13			
		PL[4]	D1	D1	D1	D1	D1	D1	D1	D1	D2	D2	D2	D2	D2	D3	D3			
A3	S8-outer	RD[3] (%)	0,26	1,15	0,51	1,17	1,92	2,63	3,44	8,25	10,31	11,25	13,13	13,13	14,69	15	16,67			
		PL[4]	D1	D1	D1	D1	D1	D2	D2	D3	D4	D4	D4	D4	D4	D4	>D4			
	S8-inner	RD[3] (%)	0,05	0,08	0,7	1,6	2,24	2,75	2,24	3,21	5,8	7,22	10,14	11,7	12,74	14,37	18,34			
		PL[4]	D1	D1	D1	D1	D2	D2	D2	D2	D4	D4	D4	D4	D4	D4	>D4			
A4	S9	RD[3] (%)	0,00	0,03	0,09	0,41	0,56	0,83	0,85	1,44	1,08	2,61	6,44	7,92	9,48	11,85	14,66			
		PL[4]	D1	D1	D1	D1	D1	D1	D1	D1	D1	D2	D3	D3	D3	D4	D4			
	S10	RD[3] (%)	0,00	0,00	0,04	0,09	0,12	0,2	0,35	0,44	0,56	1,18	4,99	6,13	7,37	8,32	9,63			
		PL[4]	D1	D1	D1	D1	D1	D1	D1	D1	D1	D1	D2	D3	D3	D3	D3			
A5 (East-Wall)	S11	RD[3] (%)	0,00	0,00	0	0,02	0,02	0,03	0,04	0,05	1,75	2,9	3,05	3,88	4,9	6,8	7,76	9,52	10,32	10,9
		PL[4]	D1	D1	D1	D1	D1	D1	D1	D1	D1	D2	D2	D2	D2	D3	D3	D3	D4	D4
	S12	RD[3] (%)	0,03	0,03	0,03	0,03	0,04	0,04	0,05	0,06	0,06	0,07	0,08	0,1	0,11	0,12	0,15	0,3	1,05	0,6
		PL[4]	D1	D1	D1	D1	D1	D1	D1	D1	D1	D1	D1	D1	D1	D1	D1	D1	D1	D1
A6 (SE corner)	S13	RD[3] (%)	0,00	0,00	0	0	0	0	0	0	2,12	5,11	7,3	11,54	19,32					
		PL[4]	D1	D1	D1	D1	D1	D1	D1	D1	D2	D3	D3	D4	>D4					
	S14	RD[3] (%)	0,02	0,01	0,03	0,05	0,06	0,15	0,36	0,51	0,64	1,28	2,01	3,3	4,49	5,55	7,3	6,98	9,42	11,69
		PL[4]	D1	D1	D1	D1	D1	D1	D1	D1	D1	D1	D2	D2	D2	D3	D3	D3	D3	D4
A6	S15	RD[3] (%)	0,13	0,14	0,15	0,3	1,21	2,43	3,11	5,19	8,3	8,91	14,83	24,29						
		PL[4]	D1	D1	D1	D1	D1	D2	D2	D3	D3	D3	D4	>D4						
	S16	RD[3] (%)	0,00	0,00	0	0	0,79	2,09	12,36	23,45										
		PL[4]	D1	D1	D1	D1	D1	D2	D4	D4										
	S17	RD[3] (%)	0,06	0,09	0,14	0,3	0,62	2,85	3,92	5,02	8,08	11,3	15,13							
		PL[4]	D1	D1	D1	D1	D1	D2	D2	D3	D3	D4	>D4							
	S18	RD[3] (%)	0,00	0,00	0	0	0	2,45	5,21	11,82	13,04	19,17								
		PL[4]	D1	D1	D1	D1	D1	D2	D3	D4	D4	>D4								
A7	S19	RD[3] (%)	1,38	2,65	2,71	3,02	3,37	3,77	4,08	4,56	5,11	5,55	6,08	6,76	7,19	7,74	8,29			
		PL[4]	D1	D2	D2	D2	D2	D2	D2	D2	D3	D3	D3	D3	D3	D3	D3			
	S20	RD[3] (%)	0,07	0,09	0,72	1,28	1,77	3,04	4,65	5,24	6,8	7,54	7,54	9,07	10,45	11,88	12,08			
		PL[4]	D1	D1	D1	D1	D1	D2	D2	D3	D3	D3	D3	D3	D4	D4	D4			
	S21	RD[3] (%)	0,01	0,01	0,15	0,28	0,54	0,96	1,93	4,94	5,5	7,47	7,47	8,19	9,19	10,79	12,25			
		PL[4]	D1	D1	D1	D1	D1	D1	D1	D2	D3	D3	D3	D3	D3	D4	D4			

(1)NSL: Normal Static Loading, (2)HHL: High Hydrological Load, (3)RL: Relative Drift, (4)PL: Performance Level

Figure 9. Incremental pseudo-static seismic procedure ("pushover-like"): stepwise increase of control acceleration and mapping of response to D-levels. Performance level color coding: Green D1, Yellow D2, Orange D3, Red D4 and Purple is exceedance of D4. Adapted from GEO.PER. S.A. & DOMOS S.A., 2023.

Cross-checks: dynamic analyses and staged mechanical-history calibration

Pseudo-static analysis is an approximation; its reliability is strengthened by two targeted cross-checks documented in the geotechnical report:

- Dynamic time-history SSI analyses were executed for two contrasting sections (S9 and S10), using the Parnitha 1999 earthquake recording at Syntagma Square (Metro station record). The record was scaled so that its PGA corresponds to a target pseudo-static effective acceleration aeff = 0.16 g (Psycharis, 2015; Stavrakakis, 2009; GEO.PER. S.A. & DOMOS S.A., 2023). These representative 2D cross-check analyses formed part of the broader pseudo-static numerical investigation described above.
- Staged pseudo-static "mechanical-history" analyses were used to interpret observed pathology and to calibrate key parameters (notably interface behaviour and degradation assumptions) against historically plausible sequences of loading and interventions (GEO.PER. S.A. & DOMOS S.A., 2023).

- A rainwater scenario is represented in the staged framework as temporary saturation/pressure effects during intense rainfall events, expressed in the report through indicative pore-pressure proxies (e.g., RU ≈ 0.10 and small hydrostatic pressures within interfaces) (GEO.PER. S.A. & DOMOS S.A., 2023).

Additional analyses

To better assess the seismic response of certain critical areas of the Circuit Wall (A1 and A5), 3D nonlinear soil–structure interaction dynamic analyses were performed considering the coupled behaviour of the wall, the foundation rock mass, and the retained embankments. These characteristic areas required further investigation because abrupt geometric variations in section and alignment do not permit the assumption of plane-strain conditions. Representative 3D simulation outputs for Areas A1 and A5 are shown in Figures 10 and 11, respectively.

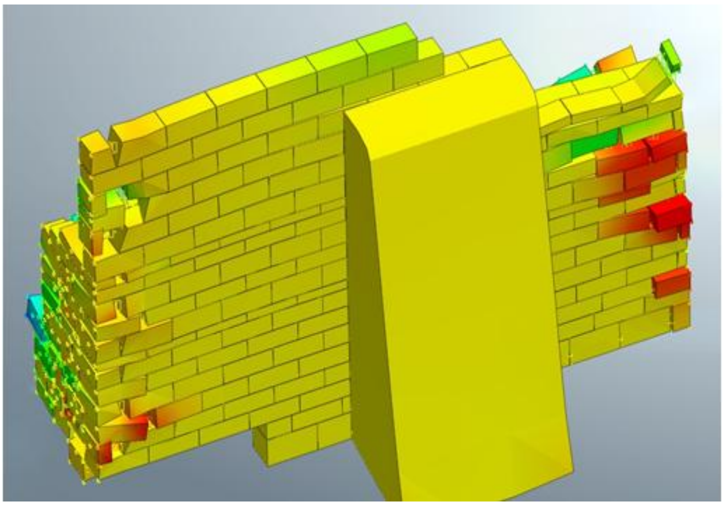

Figure 10. Simulation for 3D analysis in Area A1 (North Wall)

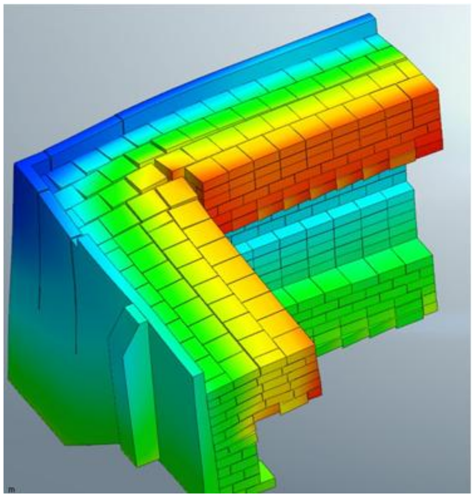

Figure 11. Simulation for the 3D analysis at the SE corner of the Wall (Area A5)

CURRENT CONDITION RESPONSE AND ILLUSTRATIVE RESULTS

Gravity and rainwater effects

Under normal geostatic loading, many cross-sections exhibit stable behaviour, consistent with long-term survival. Controlling vulnerabilities vary: some sections are governed by outward rotation potential, others by localized deformation in thin wall zones, and still others by sensitivity to transient rainwater infiltration, temporary water accumulation behind the wall, and interface shear strength (GEO.PER. S.A. & DOMOS S.A., 2023).

Intense rainfall effects can be represented through simplified transient pore-pressure assumptions or equivalent thrust increases where detailed seepage data are not available, acknowledging that the purpose is comparative assessment rather than a definitive hydraulic reconstruction (GEO.PER. S.A. & DOMOS S.A., 2023).

Incremental pseudo-static seismic response (“pushover” curves)

Incremental pseudo-static results are expressed as curves of normalised top displacement versus effective acceleration, with intersections against D-level thresholds marking the acceleration capacity associated with each damage/performance level. This corresponds directly to the “quasi pushover” use of the 0.02 g step scaling described in the report (GEO.PER. S.A. & DOMOS S.A., 2023). Representative pseudo-pushover curves for Sections S11, S13, S17 and S18 are shown in Figure 12.

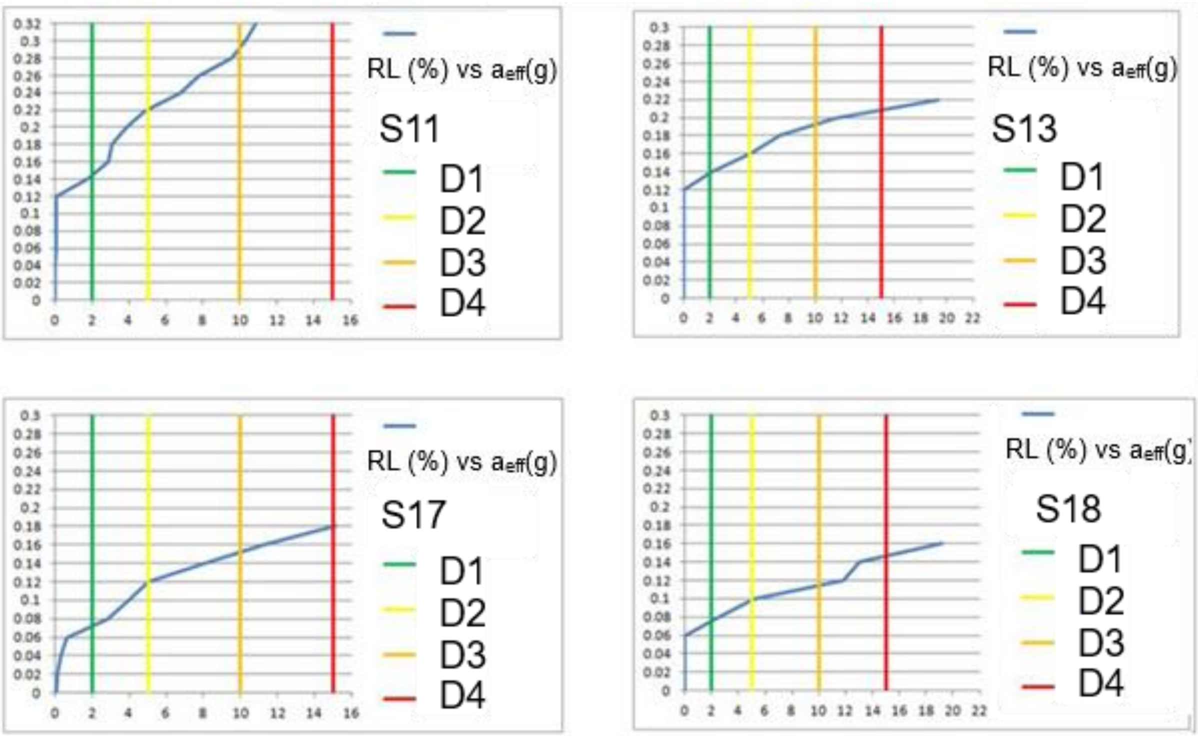

Figure 12. Incremental pseudo-static performance evolution curve for cross-sections S11, S13, S17 & S18 (pseudo-pushover). Relative Displacement versus effective acceleration, with color coded upper limits D1–D4 for relative displacements (Green D1, Yellow D2, Orange D3 and Red D4. Adapted from GEO.PER. S.A. & DOMOS S.A., 2023.

Dynamic vs pseudo-static comparison and interface-strength sensitivity

Dynamic SSI analyses were used as an explicit cross-check of the pseudo-static screening methodology: Section S9 (discontinuous/discrete structure) and Section S10 (monolithic "newer" masonry). Dynamic analyses employed the 1999 Parnitha earthquake recording from the Syntagma Square (Metro) station, scaled so that the input (PGA=0.24 g) corresponds to a_{eff} = 0.16 g in the pseudo-static framework (GEO.PER. S.A. & DOMOS S.A., 2023). The accelerogram components of the adopted seismic input are presented in Figure 13.

At a_{eff} = 0.16 g, the comparison reported:

- S9 (discrete structure): computed relative top displacement 0.18 m in both dynamic and pseudo-static analyses (GEO.PER. S.A. & DOMOS S.A., 2023).

- S10 (quasi monolithic mortared masonry structure): computed relative top displacement 0.08 m (pseudo-static) versus 0.06 m (dynamic), consistent with the typical tendency of pseudo-static procedures to be conservative for permanent displacement prediction (GEO.PER. S.A. & DOMOS S.A., 2023).

A second set of analyses for S9 examined sensitivity to residual interface friction (reduced "remaining" friction values) because the location has a documented history of failure. Under reduced interface friction, the response escalated to displacement levels consistent with computational collapse: 0.74 m (dynamic) and 0.96 m (pseudo-static), with sliding concentrated near the second course above the base, i.e., a kinematic pattern aligned with interface-governed sliding in a discrete wall (GEO.PER. S.A. & DOMOS S.A., 2023).

This paired evidence is not a generic "uncertainty statement": it identifies a controlling parameter (interface friction), demonstrates its leverage on the response in a representative discontinuous section, and supports a specific intervention emphasis—reduce seismic thrust and prevent rainwater-driven reduction of effective stress at interfaces—rather than attempting to "strengthen the monument" in a modern structural sense (GEO.PER. S.A. & DOMOS S.A., 2023).

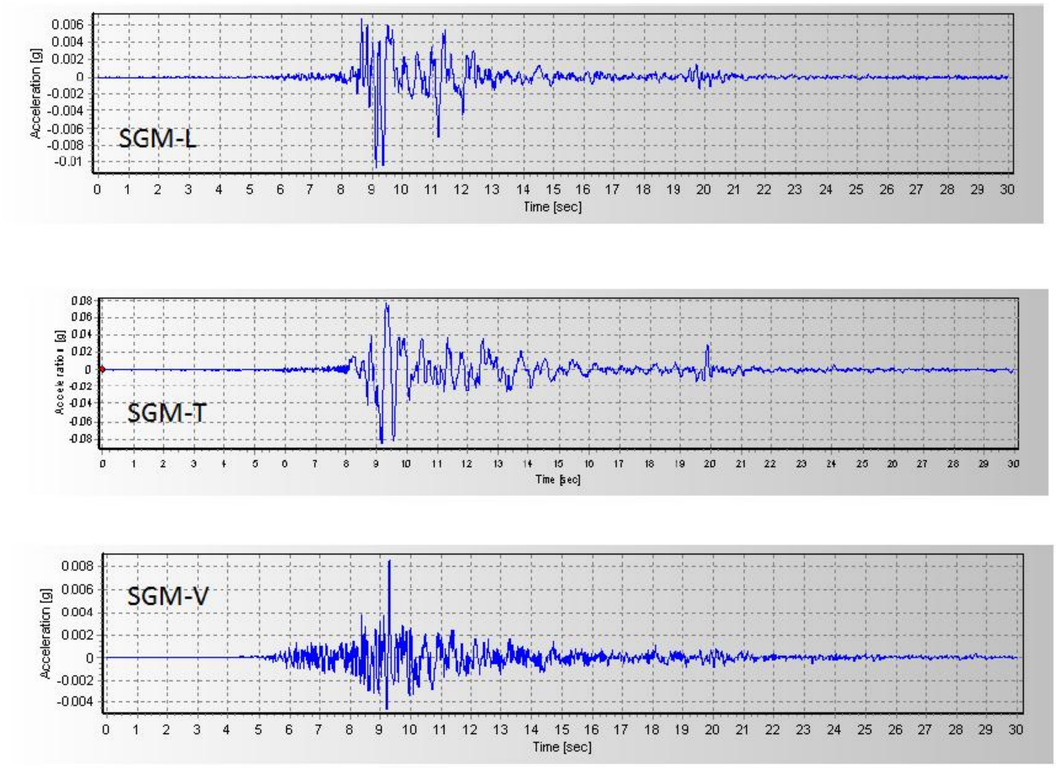

Figure 13. Accelerogram components of seismic actions during 1999 Parnetha event in metro station Syntagma. Adapted from (GEO.PER. S.A. & DOMOS S.A., 2023). Original Data from: ITSAK (Itsak, 2019)

UNCERTAINTIES AND LIMITATIONS

Uncertainties

Under geostatic conditions, the Acropolis Wall exhibits stable behaviour. Under seismic loading, however, several Areas exceed acceptable damage levels, particularly where retaining action combines with unfavourable geometry or degraded masonry.

For a multi-phase monument such as the Circuit Wall, uncertainty is not an abstract disclaimer; it directly controls which mitigation strategy is justified. The dominant uncertainty sources are:

- Internal build-up and discontinuities (unknown stone arrangement, hidden voids, variable bonding), which determine whether a section behaves as a quasi-monolith or as a discrete block system (Korres, 2015; GEO.PER. S.A. & DOMOS S.A., 2023)

- Interface shear parameters (between wall courses, between wall and rock, between wall and backfill), which were shown—by explicit sensitivity analysis—to govern whether a discrete section remains in moderate displacement or transitions to collapse-consistent kinematics (Section 6.3) (GEO.PER. S.A. & DOMOS S.A., 2023).

- Rainwater boundary conditions (short-duration saturation, ponding, and pressure build-up during intense rainfall events), which can temporarily reduce effective stress and amplify thrust. In the staged framework this is represented through indicative pore-pressure proxies and interface pressure assumptions associated with an intense rainfall event (e.g., RU ≈ 0.10 and interface pressure p ≈ 1 kPa) (GEO.PER. S.A. & DOMOS S.A., 2023).

- 2D idealisation and geometric transitions, which may be non-conservative near abrupt plan changes (corners, buttresses, sharp changes in retained height), motivating the use of targeted 3D checks where geometry demands it (GEO.PER. S.A. & DOMOS S.A., 2023).

How uncertainty is managed in the assessment framework

Three elements of the methodology directly respond to these uncertainties:

- Incremental pseudo-static scaling (0.02 g increments from 0.02 g upward) provides a capacity-type description rather than a single pass/fail point. It allows each section to be ranked by the acceleration at which D-level thresholds are reached, and it reduces dependence on selecting specific accelerograms for screening across many sections (GEO.PER. S.A. & DOMOS S.A., 2023).

- Typology-based dynamic cross-checks are used to test whether pseudo-static screening is consistent with time-history behaviour in representative “end-member” typologies: a discrete/discontinuous section (S9) and a monolithic section (S10). The close agreement at aeff = 0.16 g for S9 and the modest pseudo-static conservatism for S10 establish the pseudo-static procedure as a defensible screening tool for permanent displacement—while the reduced-interface-friction sensitivity case establishes the lever arm of interface uncertainty and its consequence (GEO.PER. S.A. & DOMOS S.A., 2023).

- Staged mechanical-history calibration is used to anchor parameter choices to observed damage patterns and plausible historical loading sequences, rather than treating parameter selection as arbitrary. The report explicitly frames these staged analyses as tools for interpreting pathology and calibrating geotechnical/geostatic parameters for present-condition analyses (GEO.PER. S.A. & DOMOS S.A., 2023).

The practical implication is that the numerical model is not presented as a “single truth.” Instead, it is used as a structured instrument for (i) ranking sections, (ii) identifying controlling mechanisms, and (iii) choosing measures that remain effective under the dominant uncertainty drivers (interfaces and rainwater effects) (Egglezos et al., 2022)

INTERVENTION STRATEGY AS BUNDLES

Intervention bundles

Intervention options are organised as Bundles (B) to align heritage constraints with mechanism control. The guiding principle is to privilege action-reduction and boundary-condition improvement (geotechnical and rainwater management measures) over invasive strengthening of historic masonry.
The intervention bundles are presented in Table 3. An example of the mapped restoration zones in later mortared masonry is shown in Figure 14.

Table 3. *Intervention Bundles B1–B8: targeted mechanisms, and implementation*

	Bundle	Targeted Mechanisms	Implementation
B1	Rainwater management and hydro-mechanical control	Temporary thrust amplification due to intense rainfall; transient pore-pressure increase; reduction of effective stress at interfaces	Includes local drainage enhancement, water-path control, prevention of ponding; priority in sections sensitive to interface friction degradation
B2	Selective consolidation of deteriorated masonry	Localized material degradation; reduced compressive or shear resistance in outer leaves	Re-bedding, repointing, limited stone replacement; applied only where pathology controls mechanism
B3	Interface improvement (wall–rock; critical joints)	Sliding at degraded interfaces; loss of shear transfer in discontinuous masonry	Local shear-transfer restoration, compatible anchoring or detailing; critical in sections analogous to S9
B4	Geometric correction in instability zones	Out-of-plumb geometry; eccentricity increase leading to overturning	Applied only in localized zones where geometry is the governing trigger
B5	Pressure relief and compatible	Excess seismic earth pressure; high inertial thrust in retaining	Controlled excavation and replacement with self-supporting dry-stone/pre-wall

Bundle		Targeted Mechanisms	Implementation
	backfill reconfiguration	segments	systems; principal geotechnical action-reduction measure
B6	Ground-level restoration (free-standing segments)	Loss of confinement due to historical excavation; increased slenderness	Re-backfilling to restore boundary conditions; reduces inertial demand and improves confinement
B7	Rock-mass stabilisation and anchoring	Foundation instability; differential settlement; rock wedge activation	Rock bolting, wedge stabilization, local anchoring; applied only where rock governs response
B8	Passive protection	Residual rockfall/block-fall hazard where structural upgrading is constrained	Barriers, catch systems, protective screens; used where performance targets cannot be structurally achieved

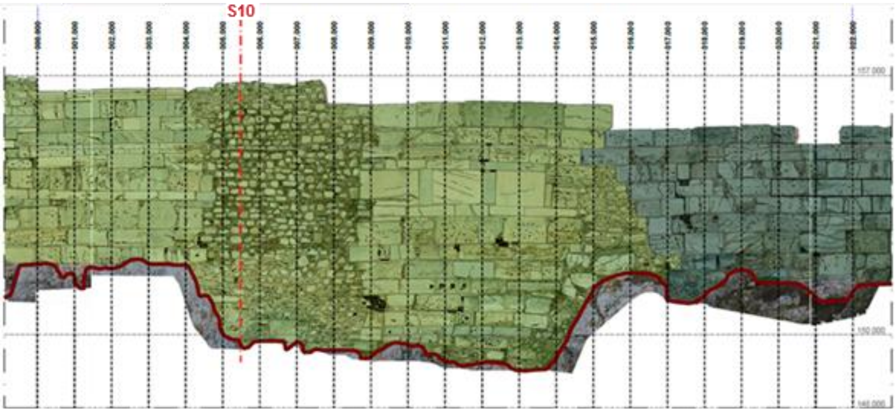

Figure 14. Later stonework with mortar (reconstruction) of the eastern section of the Circuit Wall of the Acropolis (Light cyan area: Replacements and/or supplements with new material, Light green area Restorations with new mortar and stone, Red line Local restoration interventions at the footing of the wall)

Mechanism-to-bundle mapping

Bundles are selected per Area (A) by mapping computed controlling mechanisms (rotation, interface sliding, local plasticity, rainwater amplification) to the smallest compatible bundle set that raises the acceleration capacity associated with D2–D3 damage level, without altering the monument's structural concept (Egglezos et al., 2022; GEO.PER. S.A. & DOMOS S.A., 2023). Representative sections corresponding to Bundles B5 and B6 are shown in Figures 15 and 16, respectively, while additional examples of the proposed footing-anchor arrangement and passive rock-fall protection are presented in Figures 17 and 18.

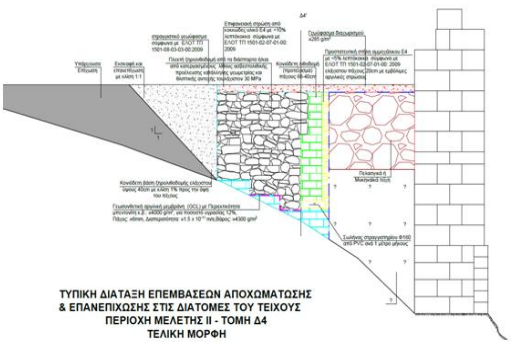

Figure 15. Typical section with intervention measures to improve stability (Bundle B5) in Area A2 (GEO.PER. S.A. & DOMOS S.A., 2023).

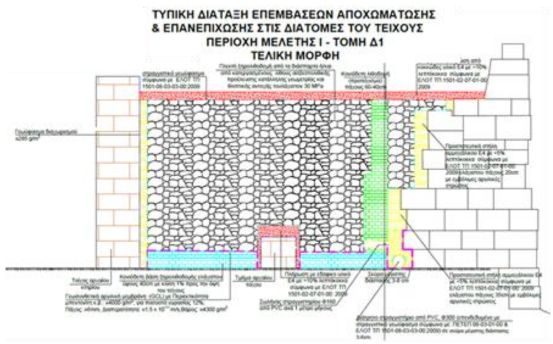

Figure 16. Typical section with intervention measures to improve stability (Bundle B6) in Area A1 (GEO.PER. S.A. & DOMOS S.A., 2023).

Figure 17. Front view of the Acropolis Wall in area A1. Suggesting location for Footing Anchors (B7). Adapted from GEO.PER. S.A. & DOMOS S.A., 2023.

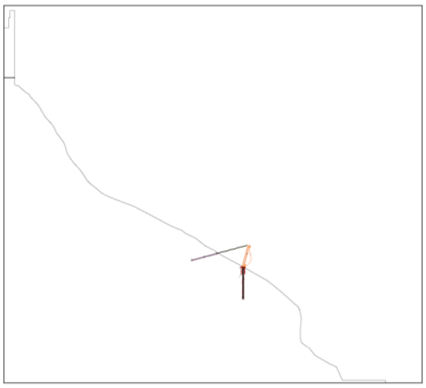

Figure 18. Typical section of passive rock-fall protection measures (B8). Adapted from GEO.PER. S.A. & DOMOS S.A., 2023).

Analyses for measure justification

Similar to the assessment of the current condition of several cross-sections of the Circuit Wall, the effect of the proposed intervention measures on stability was evaluated through staged two-dimensional elastoplastic analyses under the seismic action corresponding to the extreme design earthquake as defined by Eurocode 8. The return period of the regulatory seismic action is T_R=1300 years.

More specifically, the analyses include the following computational stages: Existing condition excavation and soil removal (where the circuit wall operates statically as a retaining wall), construction of the mortared rubble-stone foundation structure, construction of the mortared forewall structure, construction of the self-supporting dry-stone backfill structure and the placement of granular material between the forewall and the circuit wall

Seismic loading corresponding to the extreme design earthquake was applied using importance factor γI = 1.40 (TR = 1300 years), with design accelerations ad = 0.27 g for the North Wall and ad = 0.32 g for the South Wall. The regulatory framework for the analyses and result interpretation was Eurocodes 7 and 8 (CEN 2004a; 2004b) and the Greek Code of Assessment and structural Intervention on masonry buildings (OASP, 2022).The results of the analyses include, among others: computed horizontal displacement, stress state expressed in terms of principal stresses and cracking zones represented by plastic strain localization in both the circuit wall and the forewall under the extreme design earthquake action. Representative results illustrating the performance response of the circuit wall are presented in Figures 19 and 20.

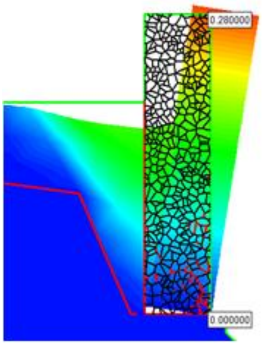

Figure 19. Computational horizontal displacement of the cross-section S10 for the extreme earthquake (TR=1300 years) after structural reinforcement (Bundles B3 and B4) and Computational cracking zones at the mortar joints (red color)

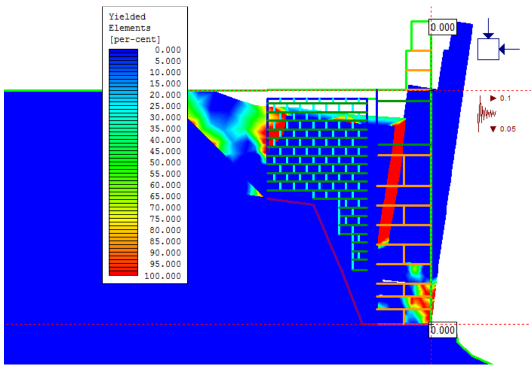

Figure 20. Computational cracking zones in the structures of section S9 for the extreme earthquake (TR=1300 years) following geotechnical interventions (Bundle B5). Color Spectrum Legend: BLUE = Elastic region, RED = Completely plastic (= fully cracked region).

DISCUSSION AND CONCLUSIONS

The incremental pseudo-static procedure (0.02 g step scaling) provides a common performance axis—effective acceleration—across heterogeneous wall typologies. This supports consistent ranking of cross-sections by the acceleration at which D-level thresholds are reached, and it avoids presenting performance as a binary “safe/unsafe” judgement that would be unjustified under the known uncertainties (GEO.PER. S.A. & DOMOS S.A., 2023).

The dynamic cross-checks using the 1999 Parnitha earthquake record (Syntagma Square station) confirm that pseudo-static screening can approximate permanent displacement demand in representative typologies when the input is scaled to a comparable effective acceleration (aeff = 0.16 g). Specifically, the reported displacement agreement for S9 (0.18 m both ways) and the modest pseudo-static conservatism for S10 (0.08 m vs 0.06 m) support the pseudo-static approach as a practical screening tool (GEO.PER. S.A. & DOMOS S.A., 2023).

The same dataset also demonstrates why the intervention strategy is formulated as dominantly geotechnical minimum intervention rather than as “structural upgrading.” When interface friction is reduced to residual values in the discrete section S9, predicted displacements rise to collapse-consistent levels (0.74–0.96 m) with a clear sliding mechanism near the base courses (GEO.PER. S.A. & DOMOS S.A., 2023). This behaviour is governed less by “lack of strength of the masonry” than by (i) interface shear transfer, and (ii) lateral thrust, both of which can be addressed more compatibly by acting on the surrounding ground and boundary conditions.

Accordingly, the central mitigation concept is to reduce seismic demand and stabilise boundary conditions through measures that are inherently aligned with conservation principles:

- Rainwater management (B1) targets temporary thrust amplification during intense rainfall by improving drainage and preventing local water accumulation behind the wall, without altering historic fabric beyond local detailing (GEO.PER. S.A. & DOMOS S.A., 2023).

- Pressure relief and compatible backfill reconfiguration (B5) reduces seismic earth pressures by replacing adverse retained soil configurations with self-supporting dry-stone systems (and where required pre-wall constructions), preserving gravity behaviour and avoiding intrusive structural frames (Egglezos et al., 2022; GEO.PER. S.A. & DOMOS S.A., 2023).

- Ground-level restoration (B6) reinstates confinement/protection in free-standing zones created by historic excavations, addressing long-term deterioration drivers while also improving seismic response by restoring boundary conditions (GEO.PER. S.A. & DOMOS S.A., 2023).

- Rock-mass stabilisation (B7) limits foundation-driven distress where rock conditions dominate risk, again focusing on boundary-condition control rather than on altering the monument’s visible structure (GEO.PER. S.A. & DOMOS S.A., 2023).

- Selective masonry work (B2–B4) remains important, but it is framed as local capacity restoration where deterioration is controlling, not as a general strengthening programme. Where constraints prevent reaching target performance, passive protection (B8) is used for consequence reduction (YSMA, 2020)

Overall, the Circuit Wall is best treated as a spatially variable geo-structural system. A performance-based workflow combining nonlinear SSI modelling, deformation-based D-level criteria, incremental pseudo-static capacity description, typology-based dynamic cross-checks, and staged mechanical-history calibration provides a defensible basis for prioritising interventions that are minimally invasive because they primarily reduce actions, rather than introducing new structural systems into the historic fabric (GEO.PER. S.A. & DOMOS S.A., 2023).

Table 4. *Regulatory Seismic response of the Athenian Acropolis Circuit Wall, in the studied areas, in current condition and post-intervention.*

Area	Section	Bundles B1	B2	B3	B4	B5	B6	B7	B8	Existing Condition (EC-8)	Post-Intervention (EC-8)
A1	S1	✓	✓	✓	✓		✓	✓		D1/D2	D1
A2	S4	✓	✓	✓	✓	✓				D4	D1
A3	S8	✓	✓	✓	✓	✓		✓	✓ (4)	FAILURE	D2
A4	S9 (1)	✓	✓	✓	✓			✓		D4	D1
A4	S10 (2)	✓	✓	✓	✓			✓	✓ (4)	D3	D2
A5	NW CORNER (3)	✓	✓	✓	✓					D1/D2	D1
A6	S6	✓	✓	✓	✓	✓		✓	✓	FAILURE (5)	FAILURE
A7	S19–S21	✓	✓	✓	✓					D3/D4	D3

(1) Ancient dry structure, (2) Newer mortar bound stonework, (3) 3D Model, (4) Temporary rock-fall barrier, (5) Computational Failure at a_g=0.18g after measure implementation against a_g=0.12g prior measure implementation.

ACKNOWLEDGEMENTS

The author would like to express his sincere appreciation to the Service for the Restoration of the Acropolis Monuments (YSMA) for the excellent cooperation and continuous institutional support provided throughout the investigation and implementation phases of the studies that provided the technical basis for the present paper. The author also gratefully acknowledges the Committee for the Conservation of the Acropolis Monuments (ESMA) for its fruitful scientific collaboration, constructive input, and creative exchange of views, which were instrumental to the successful completion of the studies within the strict framework of monument protection.

The author also expresses his appreciation to Mr Manolis Tzannidakis, Civil Engineer (MSc), for his support in preparing the illustrative material and formatting the manuscript, as well as for his constructive comments and practical suggestions that improved clarity and presentation.

REFERENCES

Ambraseys, I. N. (2010). On the long-term seismicity of the city of Athens.

Bundgaard, J. A. (1974). The Excavation of the Athenian Acropolis, 1882–1890. Copenhagen.

CEN (2004a). EN 1997-1 Eurocode 7: Geotechnical design – Part 1: General rules. European Committee for Standardization, Brussels.

CEN (2004b). EN 1998-1: Eurocode 8: Design of structures for earthquake resistance—Part 1: General rules, seismic actions and rules for buildings. European Committee for Standardization, Brussels.

CEN (2004c). EN 1998-5: Eurocode 8: Design of structures for earthquake resistance—Part 5: Foundations, retaining structures and geotechnical aspects. European Committee for Standardization, Brussels.

Coulomb, C. A. (1776). *Essai sur une application des règles des maximis et minimis à quelques problèmes de statique relatifs à l'architecture*. Paris: Académie Royale des Sciences.

Chen, W. F., & Mizuno, E. (1990). *Nonlinear analysis in soil mechanics: Theory and implementation*. Elsevier.

Duncan, J. M., & Wright, S. G. (2005). *Soil strength and slope stability*. John Wiley & Sons.

Egglezos, D., et al. (2019). Seismic behaviour of the perimeter wall of the Acropolis of Athens: Assessment of the existing condition and ways to improve the seismic response. In Proceedings of the 4th Panhellenic Conference on Earthquake Engineering and Engineering Seismology, Athens, Greece (in Greek).

Egglezos, D., & Moullou, D. (2022). Documentation of strong earthquakes of the 18th century in connection with structural damage to the Circuit Wall of the Acropolis of Athens. In Proceedings of the 5th Hellenic Conference on Earthquake Engineering and Engineering Seismology (in Greek)..

Egglezos, D., Papadopoulos, C. Th., Papavasileiou, V., & Ioannidou, M. (2022). Permanent stabilization interventions to ensure the stability of the Acropolis of Athens Circuit wal.l In Proceedings of the 6th Restoration Conference (ΕΤΕΠΑΜ). (in Greek).

GEO.PER. S.A. & DOMOS S.A. (2018). Geotechnical–Structural Study of the Circuit Walls of the Acropolis of Athens and Their Rock Foundation in Selected Priority Areas, Stage A: Project Assessment Report. YSMA Archive (in Greek)..

GEO.PER. S.A. & DOMOS S.A. (2024). Geotechnical–Structural Study of the Circuit Walls of the Acropolis of Athens and Their Rock Foundation in Selected Priority Areas, Stage C: Application Design. YSMA Archive (in Greek)..

Hoek, E., & Brown, E. T. (1980). Empirical strength criterion for rock masses. *Journal of the Geotechnical Engineering Division, ASCE*, 106(GT9), 1013–1035.

Hoek, E., Carranza-Torres, C., & Corkum, B. (2002). Hoek–Brown failure criterion—2002 edition. *Proceedings of the North American Rock Mechanics Symposium (NARMS-TAC)*, 267–273.

Hoek, E., & Marinos, P. (2000). Predicting tunnel squeezing problems in weak heterogeneous rock masses. *Tunnels & Tunnelling International*, 32(11), 45–51.

ICOMOS (1964). International Charter for the Conservation and Restoration of Monuments and Sites (The Venice Charter). 2nd International Congress of Architects and Technicians of Historic Monuments, Venice.

ICOMOS (2003). Principles for the Analysis, Conservation and Structural Restoration of Architectural Heritage. ICOMOS General Assembly, Victoria Falls.

Institute of Engineering Seismology & Earthquake Engineering (ITSAK). (2019). *Strong motion records of the 19 July 2019 NW Attica earthquake (M5.1)*. Hellenic Strong Motion Network Database, Thessaloniki, Greece.

Kavvadias, P., & Kawerau, G. (1907). The Excavation of the Acropolis. Athens: Estia.

Korres, M. (2002). On the North Acropolis Wall. In Excavating Classical Culture: Recent Archaeological Discoveries in Greece (BAR Int. Ser. 1031), 179–186.

Korres, M. (2004). The Pedestals and the Acropolis South Wall. In A. Stewart (Ed.), Attalos, Athens and the Acropolis, 242–337.

Korres, M. (2015). The Walls of the Acropolis: Present condition and proposals for intervention. In Proceedings of the 6th International Meeting for the Restoration of the Acropolis Monuments.

Kramer, S. L. (1996). *Geotechnical earthquake engineering*. Prentice Hall.

Mohr, O. (1900). Welche Umstände bedingen die Elastizitätsgrenze und den Bruch eines Materials? *Zeitschrift des Vereins Deutscher Ingenieure*, 44, 1524–1530.

OASP. (2022). KADET – Code for assessment and structural interventions in masonry buildings. Organization for Seismic Design and Earthquake Protection, Athens.

Psycharis, I. (2015). Selection of appropriate accelerograms for dynamic analysis of the Acropolis monuments. NTUA–YSMA Technical Report (in Greek).

Rocscience. (2014). Phase2: 2D Finite Element Analysis for Rock and Soil (Version 8.0) [Computer software]. Toronto, ON, Canada: Rocscience Inc

Rocscience Inc. (2023). RS3: 3D Finite Element Method Software for Civil and Mining Applications. Toronto, Ontario, Canada.

Stavrakakis, G. N. (2009). Seismic hazard study in the area of the Acropolis. Geodynamic Institute, National Observatory of Athens (in Greek)..

YSMA Technical Office for the Walls. (2020). Strategic Intervention Plan for the Walls of the Acropolis of Athens. YSMA Archive (in Greek).